Damage Detection in Initially Nonlinear Structures based on

Variational Mode Decomposition

Yu Xin [1], Jun Li [1], Hong Hao [1,*]

[1] *Centre for Infrastructural Monitoring and Protection, School of Civil and Mechanical*
Engineering, Curtin University, Kent Street, Bentley, WA6102, Australia
Emails: yu.xin@postgrad.curtin.edu.au; junli@curtin.edu.au; hong.hao@curtin.edu.au;

Abstract: Nonlinear characteristics in the dynamic behaviors of civil structures degrade the performance of damage detection of the linear theory based traditional time- and frequency- domain methods. To overcome this challenge, the present paper proposes a damage detection approach for nonlinear structures based on Variational Mode Decomposition (VMD). In this approach, the measured dynamic responses from nonlinear structures under earthquake excitations are adaptively decomposed into a finite number of mono-components by using VMD. Each decomposed mono-component represents an amplitude modulated and frequency modulated (AMFM) signal with a limited frequency bandwidth. Hilbert transform is then employed to identify the instantaneous modal parameters of the decomposed mono-modes, including instantaneous frequencies and mode shapes. Based on the identified modal parameters from the decomposed structural dynamic responses, two damage indices are defined to identify the location and severity of structural damage, respectively. To validate the effectiveness and accuracy of the proposed approach, a nonlinear seven-storey shear building model with four different damage cases under earthquake excitations is used in the numerical studies. In experimental verifications, data from shake table tests on a 12-storey scaled reinforced concrete frame structure with different earthquake excitations are analysed with the proposed approach. The results in both numerical studies and experimental validations demonstrate that the proposed approach can be successfully applied for nonlinear structural damage identification.

Keywords: Variational Mode Decomposition, Initially nonlinear structure, Earthquake excitation, Damage identification, Instantaneous modal parameters, Damage index

* Corresponding author, John Curtin Distinguished Professor Hong Hao, Centre for Infrastructural Monitoring and Protection, School of Civil and Mechanical Engineering, Curtin University, Kent Street, Bentley, WA6102, Australia. Email: hong.hao@curtin.edu.au

1. Introduction

Civil engineering structures may accumulate local or global damage when subjected to extreme operational conditions, i.e. earthquakes, typhoons, and other extreme loading conditions. Under these circumstances, non-stationary structural dynamic responses are obtained and structural vibration characteristics vary over time. Condition monitoring based on measured structural dynamic responses is critical to assist engineers in evaluating the operational safety of structures in a cost-effective strategy. Damage detection techniques based on structural vibration responses have been widely studied in the literature [1-3]. The basic idea behind these strategies is based on the relationship between the vibration characteristics, i.e. modal parameters, and structural physical properties. Changes in structural physical parameters (i.e. structural mass, stiffness, and damping) will cause the changes in vibration characteristics. Numerous modal information based damage detection methods have been developed for linear structural damage identification in the past several decades [4-8]. However, for nonlinear structures, with the nonlinear characteristics due to the hysteretic stiffness and damping force, structural vibration characteristics of these structures cannot be predicted accurately by using the linear theory and the traditional time domain and frequency domain methods. Since the real-world structures may have nonlinear behavior even under the healthy state, to detect the existing structural damage under the effect of initially nonlinearity based on the linear theory is not feasible and accurate.

In recent years, damage detection and time-varying/nonlinear system identification by using the time-frequency analysis techniques have received significant attention. Various time-frequency analysis methods reported in the literature [9-10] include Short-time Fourier transform (STFT), Wigner-Ville distribution (WVD), Wavelet Transform (WT) and Hilbert-Huang Transform (HHT).

Among these mentioned time-frequency presentation methods, the WT and HHT methods may be the two most popular time-frequency analysis tools, which have been applied to track the varying dynamic behavior of structures subjected to external excitation. For instance, Ruzzene et al. [11] used complex WT to estimate natural frequencies and viscous damping ratios from structural dynamic responses under ambient vibrations. Xin et al. [12] proposed an improved Empirical Wavelet transform (EWT) approach for time-varying system identification, and the method was successfully applied to track the varying dynamic characteristics of a highway bridge under heavy traffic loads. Daubechies et al. [13] developed a synchrosqueezed wavelet transform (SSWT) method for system identification, which significantly improved the time frequency resolution of classical wavelet transform and enabled precise signal reconstruction. HHT is an alternative time-frequency representation technique, which was first introduced for the signal processing of non-linear and non-stationary processes by Huang et al. [14, 15]. Wang et al. [16] proposed a recursive HHT method to identify the time-varying dynamic properties of shear-type building structures under base excitations. Bao et al. [17] developed an improved HHT algorithm for non-stationary and nonlinear dynamic response analysis with closely spaced modes. However, the mode mixing still exists when using HHT method for strong non-stationary signal analysis. More recently, a novel adaptive filter algorithm, Variational Mode Decomposition (VMD) has been developed [18] and successfully applied for signal decomposition and instantaneous frequency identification of stationary/non-stationary signals [19-21].

For nonlinear or time-varying systems, the identified instantaneous modal parameters, i.e. instantaneous natural frequency and mode shape, can be further employed to evaluate structural damage. For instance, Ditommaso et al. [22] designed an S-Transform based band-variable filter for

non-stationary signal decomposition, and then the modal curvature of the decomposed fundamental mode shape was derived for structural damage localization of time varying structures. In Ref. [23], the degree of nonlinearity was considered as a damage index to evaluate the damage of structures by using Hilbert transform.3 In addition, the SSWT method was employed to identify the instantaneous modal parameters of the time-varying structures subjected to external excitations [24], and the identified instantaneous modal parameters were further used to construct a time-varying damage index.

In this study, the VMD method with Hilbert transform is applied for instantaneous modal parameter identification of nonlinear structures subjected to seismic excitations. The identified modal parameters of the decomposed mono-components are further employed to define two damage indices for damage localization and quantification of nonlinear structures. Responses of a nonlinear seven-storey shear building structure with four damage cases subjected to earthquake excitations are calculated and analyzed to demonstrate the feasibility of the proposed approach. Experimental verifications are conducted with the benchmark testing data on a shake table test of a 12-storey scaled reinforced concrete (RC) frame structure to demonstrate the efficiency and performance of the proposed nonlinear structural damage identification approach. Although the VMD method and Hilbert transform have been successfully used for instantaneous parameter identification in Ref. [20], the innovation of this work is mainly on extending the identified instantaneous parameters for nonlinear structural damage detection based on the defined damage indices.

The remainder of this paper is organized as follows. In section 2, the background of the VMD method and Hilbert transform is first introduced, and then, two developed damage indices based on the identified instantaneous modal parameters are described. Numerical studies on a seven-storey

5

nonlinear shear building structure with various damage conditions subjected to earthquake excitations are applied to verify the feasibility of using the proposed damage indices for nonlinear structural damage identification in Section 3. Then measurement data from shake table tests on a scaled RC frame structure under earthquake excitations are used to further validate the capability of the proposed approach in Section 4. Finally, the conclusions are summarized in Section 5.

2. Theoretical Background

2.1. Instantaneous modal parameters identification based on VMD

For an *n* degree-of-freedom (DOF) nonlinear system subjected to ground motions, the equation of motion of the system can be written as

$$M\{\ddot{x}(t)\} + F_c\{\dot{x}(t)\} + F_s\{x(t)\} = -ML\ddot{x}_g(t) \tag{1}$$

where the mass matrix is defined by M, $F_c\{\dot{x}(t)\}$ and $F_s\{x(t)\}$ denote the damping force and the nonlinear restoring force vectors, respectively; $x(t)$, $\dot{x}(t)$ and $\ddot{x}(t)$ represent the displacement, velocity and acceleration response vectors of the nonlinear system; $\ddot{x}_g(t)$ is the applied ground motion record, and L denotes the mapping vector of the applied excitation to the associated DOFs of the structure. For a nonlinear structure, Equation (1) can also be further transformed into [25]

$$M(t)\ddot{x}(t) + C(t)\dot{x}(t) + K(t)x(t) = -ML\ddot{x}_g(t) \tag{2}$$

in which, $M(t)$, $K(t)$ and $C(t)$ denote the time-varying mass, stiffness and damping matrices of the nonlinear structure, respectively. In Equation (2), since structural dynamic responses consists of several individual components $x^{(i)}(t)$ with time-varying frequencies and amplitudes [25], the vibration signals $x(t)$ can be further expressed as a combination of these individual components

$$x(t) = \sum_{i=1}^{n} x^{(i)}(t) \tag{3}$$

For a nonlinear structure, the frequency components may change with time during structural vibration. The VMD with an adaptive filter [18] can be performed to decompose the individual

components from the structural vibration signals. The theoretical background is briefly described herein.

The signal decomposition using VMD method can be considered as a constrained variational problem, and the corresponding objective function is described as

$$f_{obj} = \min_{\{x^{(i)}\}\{\overline{\omega}_i\}} \left\{ \sum_{i=1}^{m} \left\| \partial_t \left[\left(\delta(t) + \frac{j}{\pi t} \right) * x^{(i)}(t) \right] e^{-j\overline{\omega}_i t} \right\|_2^2 \right\} \tag{4}$$

subjected to

$$x(t) = \sum_{i=1}^{m} x^{(i)}(t) \tag{5}$$

in which * is the convolution symbol, δ denotes the Dirac function, $\{x^{(i)}\} = \{x^{(1)}, x^{(2)}, \ldots, x^{(m)}\}$ and $\{\overline{\omega}_i\} = \{\overline{\omega}_1, \overline{\omega}_2, \ldots, \overline{\omega}_m\}$ represent the different modes of the target signal $x(t)$ and the corresponding center frequencies, respectively.

By using the Lagrangian multipliers λ and a quadratic penalty term, the optimization with the objective function in Eq. (4) can be further transferred into an unconstrained optimization problem as follows

$$L(\{x^{(i)}\}, \{\overline{\omega}_i\}, \lambda) = \beta \sum_{i=1}^{m} \left\| \partial_t \left[\left(\delta(t) + \frac{j}{\pi t} \right) * x^{(i)}(t) \right] e^{-j\overline{\omega}_i t} \right\|_2^2 + \left\| \sum_{i=1}^{m} x^{(i)}(t) - x^{(i)}(t) \right\|_2^2 +$$

$$\langle \lambda(t), x(t) - \sum_{i=1}^{m} x^{(i)}(t) \rangle \tag{6}$$

where β is the regularization coefficient, depending on the data fidelity constraint. A quadratic penalty term is introduced to accommodate the noise effect, and λ is commonly selected as the enforcement constraint. By introducing these two terms, the convergence properties and the strict enforcement of the constraints in Eq. (6) will be improved.

To solve Eq. (6), an alternate direction method of multipliers (ADMM) [26] algorithm is used. The different modes and the corresponding center frequencies of a target signal $x(t)$ can be obtained by a sequence of iterative sub-optimizations. The decomposed mode can be expressed as

$$x^{(i)}(\omega) = \frac{x(\omega) - \sum_{k \neq i} x^k(\omega) + (\lambda(\omega)/2)}{1 + 2\alpha(\omega - \bar{\omega}_i)^2} \quad (i = 1, 2, \dots, m) \tag{7}$$

in which $x^{(i)}(\omega)$ denotes the Fourier Transform (FT) of the ith mode of signal $x(t)$.

Using VMD for signal decomposition can be considered as an optimization problem, and the main process includes three steps:

Step 1: Intrinsic mode calibration.

The mode $x_{n+1}^{(i)}(\omega)$ is first calibrated in the spectral domain by using Eq. (8), and then $x_{n+1}^{(i)}(t)$ is obtained from the inverse FT, which is expressed as follows

$$x_{n+1}^{(i)}(\omega) = \frac{x(\omega) - \sum_{k<i} x_{n+1}^{(k)}(\omega) - \sum_{k>i} x_n^{(k)}(\omega) + (\lambda^n(\omega)/2)}{1 - 2\alpha(\omega - \bar{\omega}_i{}^n)^2} \quad (i = 1, 2, \dots, m) \tag{8}$$

$$x_{n+1}^{(i)}(t) = Re\left[\mathcal{F}^{-1}\left(x_{n+1}^{(i)}(\omega)\right)\right] \tag{9}$$

in which, the terms of $\mathcal{F}^{-1}(.)$ and $Re[.]$ denote the inverse FT and the real part of an analytic signal, respectively.

Step 2: Center frequency calibration.

The center frequency of the ith individual component $\bar{\omega}_{n+1}^{(i)}$ is the center of gravity of the corresponding mode's power spectrum, which can be expressed as

$$\bar{\omega}_{n+1}^{(i)} = \frac{\int_0^\infty \omega \left|x_{n+1}^{(i)}(\omega)\right|^2 d\omega}{\int_0^\infty \left|x_{n+1}^{(i)}(\omega)\right| d\omega} \quad (i = 1, 2, \dots, m) \tag{10}$$

Step 3: Dual ascent.

For all frequency components $\omega > 0$, the Lagrangian multipliers $\lambda^{n+1}(\omega)$ can be calculated by using the dual ascent to enforce the exact signal reconstruction until the defined convergence criteria is satisfied.

$$\lambda^{n+1}(\omega) = \lambda^n(\omega) + \tau\left(x(\omega) - \sum_i x_{n+1}^{(i)}\right) \tag{11}$$

$$\sum_{i=1}^m \frac{\left\|x_{n+1}^{(i)} - x_n^{(i)}\right\|_2^2}{\left\|x_n^{(i)}\right\|_2^2} \leq \varepsilon \tag{12}$$

The decomposed ith mono-component $x^{(i)}(t)$ by VMD can be further expressed as

$$Z^i = x^{(i)}(t) + H\left[x^{(i)}(t)\right] = A_i(t)e^{-j\theta_i(t)} \tag{13}$$

$$A_i(t) = \sqrt{x^{(i)}(t)^2 + H[x^{(i)}(t)]^2} \ , \quad \theta_i(t) = arctan\left(\frac{H\left(x^{(i)}(t)\right)^2}{x^{(i)}(t)}\right) \tag{14}$$

where $H[\ \ ]$ denotes the Hilbert transform; $A_i(t)$ and $\theta_i(t)$ are the instantaneous amplitude and phase of the analytical signal Z^i, respectively. The instantaneous frequency of the i-th component $x^{(i)}(t)$ can be obtained by calculating the derivation of $\theta_i(t)$

$$f_i(t) = \frac{d\theta_i(t)}{2\pi dt} \tag{15}$$

For structural vibrations under earthquake excitations, the identified instantaneous frequency of the nonlinear structure by Hilbert transform includes a slowly-varying frequency component and a fast-varying frequency component. Under this circumstance, the natural frequencies of the target signals are usually obtained by filtering out the fast-varying component [27-28].

2.2. Damage detection for nonlinear structures

As mentioned in a previous study [1], damage assessment can be designated to four different levels: 1) The first level is to detect whether damage has occurred; 2) The second level is to detect the damage location; 3) The third level is to identify the damage severity; and 4) The fourth level is to evaluate the remaining life of the damaged structure. Generally, a higher level of damage detection means more information and computational demand are required. To realize an effective damage identification for nonlinear structures, the third level damage detection is conducted in this study.

For civil structures under operational conditions, acceleration responses are usually easier to be measured than displacement and velocity. Therefore, nonlinear structural damage identification

9

based on the measured acceleration data will be studied in this section. **Y** is defined as a set of the measured dynamic signals from a nonlinear structure under earthquake excitations during a time period $\boldsymbol{t} = [t_1, t_2, \cdots, t_n]$, which is expressed as

$$\mathbf{Y} = \begin{bmatrix} y_1(\boldsymbol{t}) \\ y_2(\boldsymbol{t}) \\ \vdots \\ y_s(\boldsymbol{t}) \end{bmatrix} = \begin{bmatrix} y_1(t_1) & y_1(t_2) & \cdots & y_1(t_n) \\ y_2(t_1) & y_2(t_1) & \cdots & y_2(t_n) \\ \vdots & \vdots & \ddots & \vdots \\ y_s(t_1) & y_s(t_2) & \cdots & y_s(t_n) \end{bmatrix} \tag{16}$$

in which $y_s(t_n)$ denotes the measured acceleration data from the *s*-th measurement location at the time instant t_n.

VMD is performed to decompose the measured vibration signals into several individual components, which can be written as

$$\mathbf{Y}^e = \begin{bmatrix} y_1{}^{(1)}(\boldsymbol{t}) & y_1{}^{(2)}(\boldsymbol{t}) & \cdots & y_1{}^{(m)}(\boldsymbol{t}) \\ y_2{}^{(1)}(\boldsymbol{t}) & y_2{}^{(2)}(\boldsymbol{t}) & \cdots & y_2{}^{(m)}(\boldsymbol{t}) \\ \vdots & \vdots & \ddots & \vdots \\ y_s{}^{(1)}(\boldsymbol{t}) & y_s{}^{(2)}(\boldsymbol{t}) & \cdots & y_s{}^{(m)}(\boldsymbol{t}) \end{bmatrix} \tag{17}$$

where $y_s{}^{(m)}(\boldsymbol{t})$ denotes the *m*-th mono-component of the *s*-th acceleration response. When the mono-components are obtained from the measured acceleration signals, the Hilbert transform is employed to calculate the instantaneous frequencies and normalized mode shapes of the decomposed modes. The identified *i*th instantaneous modal parameters, such as instantaneous frequency and mode shape, are respectively presented as

$$\boldsymbol{\omega}^{(i)}(\boldsymbol{t}) = \left[\omega^{(i)}(t_1), \omega^{(i)}(t_2), \cdots, \omega^{(i)}(t_n) \right]^T \tag{18}$$

$$\boldsymbol{\varphi}^{(i)}(\boldsymbol{t}) = \left[\varphi_1{}^{(i)}(\boldsymbol{t}), \varphi_2{}^{(i)}(\boldsymbol{t}), \cdots, \varphi_s{}^{(i)}(\boldsymbol{t}) \right]^T \tag{19}$$

In Eq. (19), $\boldsymbol{\varphi}^{(i)}(\boldsymbol{t})$ represents the *i*th-order mode shape obtained from the measured structural dynamic responses.

Considering that the modal curvature is strongly correlated with structural damage, it has been developed for structural damage localization in previous studies [29-32]. For damage detection in

engineering structures, when the variation of modal curvature at a specific sensor location is significantly larger than those at other locations, this location can be considered as the identified damage area in structures. Therefore, based on the estimated modal curvature, a new damage index is developed for structural damage localization, which is described as follows.

Modal curvature of each mode shape can be evaluated by using the second-order central difference of the fundamental mode shape [29-30], which is described as

$$\varphi_s''^{(i)}(t_n) = \frac{\varphi_{s-1}^{(i)}(t_n) - 2\varphi_s^{(i)}(t_n) + \varphi_{s+1}^{(i)}(t_n)}{h^2} \tag{20}$$

in which $\varphi_s^{(i)}(t_n)$ denotes the ith-order mode shape of the sth location at the time instant t_n, and $\varphi_s''^{(i)}(t_n)$ is the obtained modal curvature of the ith-order mode shape; h denotes the physical distance between two adjacent sensors, and in this study it is the height of each floor when a building model is used as an example structure. Based on Eq. (20), the modal curvatures of each mode can be derived by using the time-varying normalized mode shape. The new damage index DL is defined as

$$DL_s(t_n) = \frac{1}{m}\sum_{i=1}^{m}\sqrt{\left|\left(\varphi_s''^{(i)}(t_n)\right)^2 - \left(\varphi_s''^{(i)}(t_n)\right)_{ref}^2\right|} \tag{21}$$

where the subscript 'ref' denotes the 'reference state' of a nonlinear structure, m is the number of the identified modes from structural dynamic responses. The location with the maximum value of DL can be identified as a damage location of the structure.

When the damage locations are determined based on Eq. (21), to further evaluate the damaged severity of the nonlinear structures, another damage index DQ based on the identified instantaneous modal parameters is defined, which can be expressed as

$$DQ_s(t) = 1 - \frac{\sum_{i=1}^{m}\left[\frac{\left(\varphi_s^{(i)}(t)\right)_{ref}}{\left(\omega^{(i)}(t)\right)_{ref}}\right]^2}{\sum_{i=1}^{m}\left[\frac{\varphi_s^{(i)}(t)}{\omega^{(i)}(t)}\right]^2} \tag{22}$$

in which $\varphi_s^{(i)}(t)$ is the time-variant normalized mode shape of the sth location. Based on Eq. (22), the damage severity of the nonlinear structure can be quantified by using the defined damage index *DQ* with a range from 0 (undamaged) and 1 (completely damaged). From Equations (21) and (22), it can be observed that the defined damage indices can be used to locate and quantify the time-variant damage of nonlinear structures. Fig. 1 describes the flowchart of the proposed nonlinear structural damage identification approach. Based on the process of the proposed approach, the damage localization and quantification can be simultaneously performed by using two indices *DL* and *DQ* as described in Eq. (21) and (22).
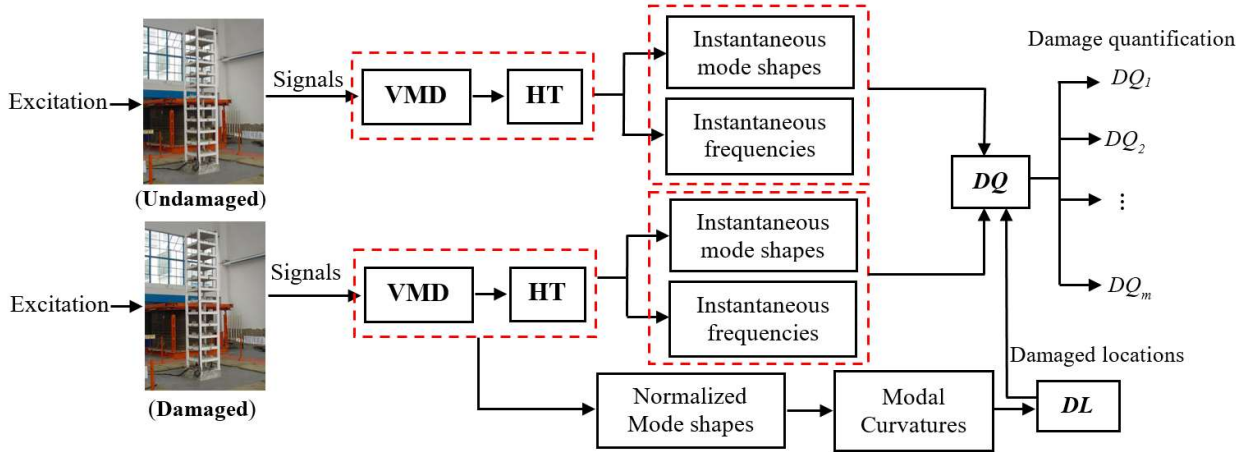
Fig. 1. Flowchart of the proposed approach (**HT** denotes Hilbert Transform)

3. Numerical Simulation

In this section, a building structure model is developed to investigate the reliability and accuracy of using the proposed approach for damage detection of nonlinear structures.

3.1 Instantaneous modal parameters identification based on VMD

In this section, a 7-DOF nonlinear shear building model, as shown in Fig. 2, is developed in MATLAB [34]. As shown in Fig. 2, the total height of the building model is 21m with 3m for each floor. In this building model, the mass m_i $(i = 1,2,\cdots,7)$ of each floor of the building is defined as 1200kg; the initial elastic stiffness k_i $(i = 1,2,\cdots 7)$ of each floor is set as $3.0{\times}10^6$ N/m, and the damping matrix element c_i $(i = 1,2,\cdots 7)$ of each floor is set as 1600N.s/m. To simulate structural nonlinear dynamic responses subjected to earthquake excitations, Bouc-Wen hysteretic models are included in each floor of the building to define the hysteretic characteristics. The equation of motion of the nonlinear structure with Bouc-Wen model [28, 35] can be expressed as

$$\mathbf{M}\ddot{\boldsymbol{u}}(t) + \mathbf{C}\dot{\boldsymbol{u}}(t) + \mathbf{K}\mathbf{z}(t) = -\mathbf{M}L\ddot{x}_g(t) \tag{23}$$

in which $\mathbf{M}$, $\mathbf{C}$ and $\mathbf{K}$ are the mass, damping and stiffness matrices of the model, respectively; $\ddot{\boldsymbol{u}}(t)$ and $\dot{\boldsymbol{u}}(t)$ represent the acceleration and velocity responses, respectively; $\mathbf{z}(t)$ denotes the hysteretic restoring force vector. $\mathbf{z}_i(t)(i = 1,2,\cdots 7)$, is the ith hysteretic restoring force and is modeled by the Bouc-Wen nonlinear differential equation [36], which is further expressed as

$$\begin{cases} \mathbf{z}_i = \dot{\boldsymbol{u}}_i - \beta_i|\dot{\boldsymbol{u}}_i|(\dot{\mathbf{z}}_i)^{n_i-1}(\mathbf{z}_i) + \gamma_i|\dot{\boldsymbol{u}}_i|(\dot{\mathbf{z}}_i)^{n_i}, (i = 1) \\ \mathbf{z}_i = \dot{\boldsymbol{u}}_i - \dot{\boldsymbol{u}}_{i-1} - (\beta_i|\dot{\boldsymbol{u}}_i - \dot{\boldsymbol{u}}_{i-1}|(\dot{\mathbf{z}}_i)^{n_i-1}(\mathbf{z}_i) + \gamma_i|\dot{\boldsymbol{u}}_i - \dot{\boldsymbol{u}}_{i-1}|(\dot{\mathbf{z}}_i)^{n_i}), (i = 2\cdots 7) \end{cases} \tag{24}$$

where β and γ are the hysteretic parameters of the Bouc-Wen model, n determines the transition from the linear to nonlinear ranges. Based on Eq. (24), it can be observed that the hysteretic force is depending on the past time history of the structural deformation. Therefore the dynamic responses of the building model are non-stationary and nonlinear under the strong external excitations.

In this simulation, the parameters of the Bouc-Wen model are set as $\beta_i = \gamma_i = 500$, $n_i = 2$, respectively. The 1940 El Centro ground motion record, shown in Fig. 3, is used as the input to the building model, and nonlinear dynamic responses of the structure are calculated by using the fourth-order Runge-Kutta method built-in MATLAB [34]. Seven accelerometers, with locations shown in Fig. 2, are assumed to record the acceleration responses in the horizontal direction of the

nonlinear building structure with a sampling rate of 50Hz. Before the dynamic analysis of the

nonlinear structure under earthquake excitations, modal parameters of the structure in the initially

linear state are obtained by using eigenvalue analysis. The first three natural frequencies of the

structure are 1.67Hz, 4.92Hz and 7.96Hz, respectively. Acceleration responses of the nonlinear

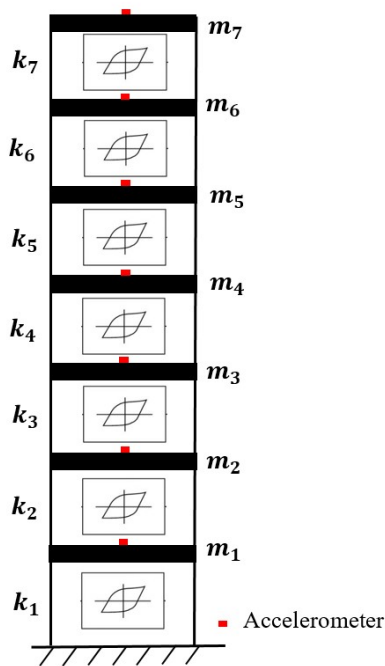model under the earthquake excitation are obtained with a time duration of 30s.

Fig. 2. A nonlinear seven-storey building structure with Bouc-Wen model.
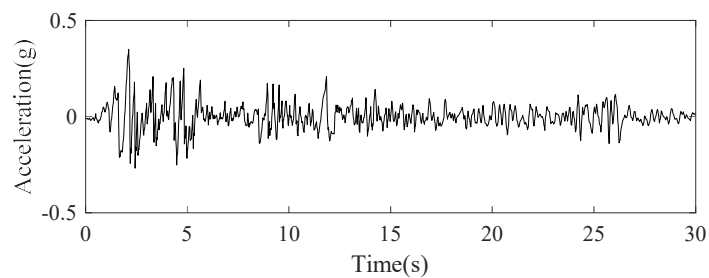
Fig. 3. The El Centro ground motion record.

Simulated acceleration responses of the shear structure model under the ground motion

excitation are used to identify the instantaneous modal parameters of the nonlinear structure with

14

the proposed approach. According to the procedure described in Section 2.1, the measured structural dynamic responses are adaptively decomposed by the VMD method, and the first two modes of the acceleration response at the top floor of the building are shown in Figs. 4(a) and (b). The Hilbert transform is then applied to identify the instantaneous modal parameters of the decomposed mono-components, which are shown in Fig. 5. It can be observed that the identified instantaneous frequencies of these two mono-components fluctuate quickly over time, and the slowly-varying frequency component can be extracted by filtering these oscillation components [27]. As observed in Figure 5, the instantaneous frequency of the signal includes fast-varying portion with significant fluctuations. This is the reason why the identified instantaneous frequencies by Hilbert transform significantly fluctuate over time, especially at the beginning of the vibrations, as shown in Figure 5. In addition, it can be seen from Figure 4 that the amplitude of the decomposed acceleration response is very small (close to zero) at the beginning of the time series, which will cause more significant fluctuations when Hilbert transform is performed. However, if the identified slowly varying frequency components in Figures 5(a) and (b) are closely observed, the initial values of natural frequencies are approximately equal to the modal analysis results of the nonlinear system. This means that the identified slowly varying frequency components can identify the time varying frequencies of the structure. The corresponding slowly-varying frequency components are shown in Fig. 5(a) and (b), respectively. They are gradually reduced during the large structural vibrations, which mean that dynamic characteristics of the nonlinear model subjected to external excitation are time-variant. The normalized mode shapes of the nonlinear structure can be identified by using the identified instantaneous amplitudes of the measured acceleration signals from seven accelerometers. The identified normalized mode shapes at 2.48s are displayed in Figs. 6(a) and (b) for the first and second modes, respectively. Once the instantaneous modal parameters of structural dynamic responses are obtained by using VMD and Hilbert transform, the proposed approach will be further used for nonlinear structural damage localization and quantification in the next section.
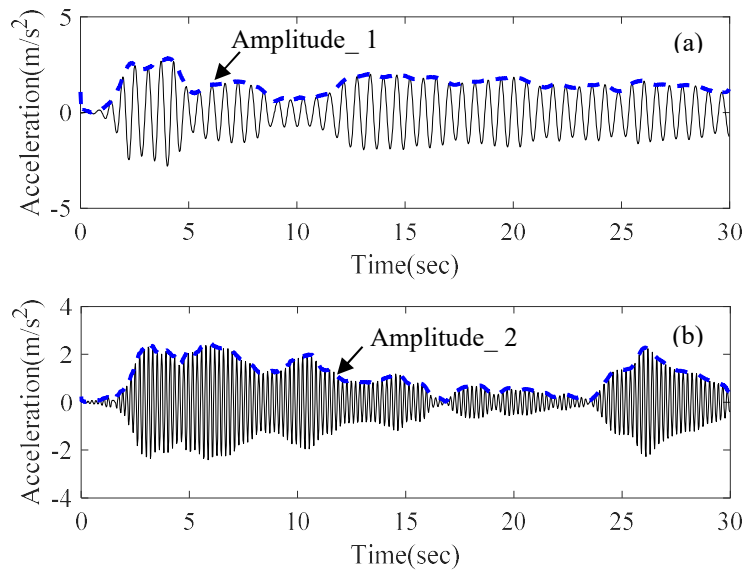
Fig. 4. Decomposed mono-components based on VMD: (a) the first component; (b) the second component.
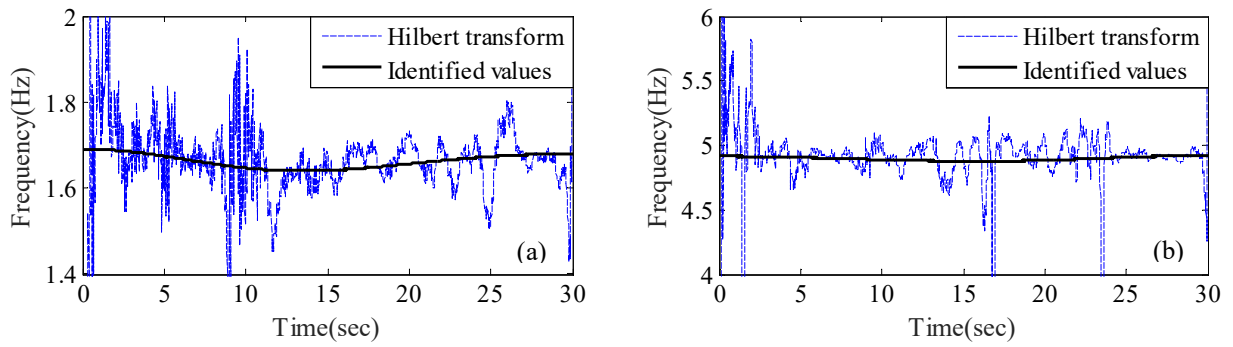

Fig. 5. Identified instantaneous frequencies based on VMD and Hilbert transform: (a) The first component; (b) The second component.
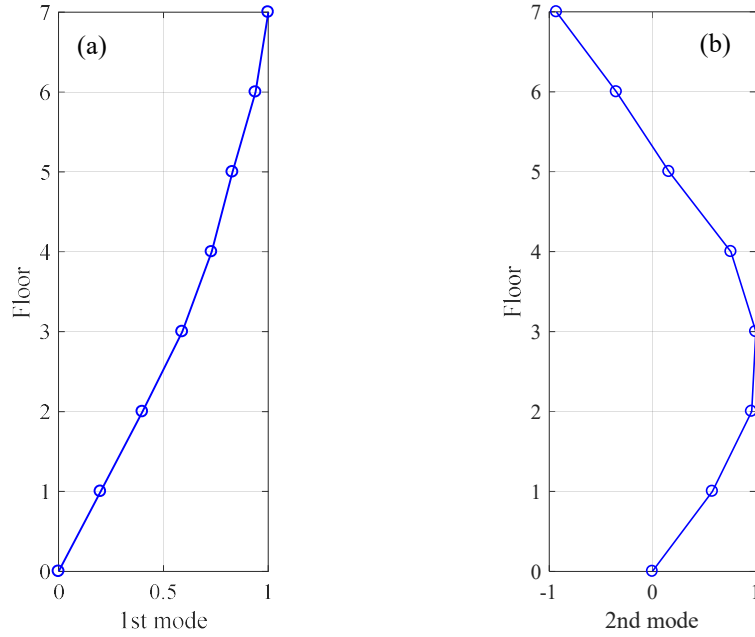
Fig. 6. Identified normalized mode shapes at 2.48 second: (a) The first mode; (b) The second mode.

3.2 Damage detection based on the instantaneous modal parameters

In this section, the identified instantaneous modal parameters are further used for damage identification of nonlinear structures. To validate the effectiveness of the proposed approach, four damage cases (Case 1 - Case 4) listed in Table 1 are assumed for this initially nonlinear building structure. As can be observed from Table 1, Cases 1 - 3 have a single damage location, but with different stiffness reduction severities and patterns. Two patterns are considered. The first one is the sudden stiffness reduction at a specific time instant, and the second one is the linear stiffness reduction over a certain time span. Two damage locations are defined in Case 4 with the both patterns. In all the damage cases, structural damage is modeled by reducing the stiffness coefficient k_i at the special floors with a certain pattern. To identify structural damage under the effects of the initial nonlinear behaviors by using the proposed approach, dynamic responses measured from the undamaged seven-storey building with nonlinear Bouc-Wen model described in

17

Section 3.1 are considered as the reference data.

Table 1. Damage cases in the numerical study

Damage Case	Damage location	Stiffness reduction
Case 1	The 2nd floor	Stiffness reduces suddenly 30% at the time instant 6s
Case 2	The 2nd floor	Stiffness reduces linearly 30% over a period from 6s to 12s
Case 3	The 2nd floor	Stiffness reduces suddenly 40% at the time instant 6s
Case 4	The 2nd floor	Stiffness reduces suddenly 30% at the time instant 6s
	The 5th floor	Stiffness reduces linearly 40% over a period from 8s to 16s

Acceleration responses of seven floors of the building under the above four damage cases subjected to the El Centro earthquake excitation are used for damage identification. In addition, to verify the performance of the proposed approach under the effect of measurement noise, 5% Gaussian white noise is added to the simulated acceleration data. The instantaneous modal parameters including natural frequencies and normalized mode shapes are respectively identified by using VMD method with Hilbert transform. Once the instantaneous frequencies and normalized mode shapes of the decomposed modes are obtained, damage identification of the nonlinear structure is conducted based on the proposed procedure as described in Section 2.2. It can be observed from Eqs. (20)- (22) that these damage indices are defined based on the identified modal parameters over time, and then damage detection can be performed during structural vibrations. Considering that the changes in the instantaneous frequency are strongly linked with structural damage severity, in this simulation, the obtained modal curvatures at the time instant of the minimum frequencies are selected for nonlinear structural damage localization. It is possible to

select more data points or all the points, however, to simplify the damage quantification process and reduce the computation demand, 15 specific data points of the instantaneous modal parameters are used to identify structural damage during vibration period. The selected point of the first component of the acceleration response from Case 1 is shown in Fig. 7, which is used for structural damage localization. Those 15 specific data points as shown in Fig. 8 are used to conduct structural damage quantification. It should be noted that the proposed approach is developed based on the obtained vibration responses, and is not a real time method.

The identified normalized mode shapes of the first decomposed component are used for nonlinear structural damage localization, while the identified two primary mono-components are applied for structural damage quantification. The normalized mode shapes identified from the instantaneous amplitudes at the time instant t_p of four damage cases are shown in Fig. 9(a), and the corresponding modal curvatures estimated by using Eq. (20) are presented in Fig. 9(b). Then, DL values of four damage cases are calculated by using Eq. (21), and the results are shown in Fig. 10. It can be observed from Fig. 10 that for the single damage cases, i.e. Case 1, Case 2 and Case 3, damage location can be determined by the maximum DL value at the 2nd floor compared with all the other sensor locations; when multiple damages are simulated, the local maximum DL values can be considered as damage locations. For Case 4, two local maximum DL values are observed at the 2nd and 5th floors. These results indicate that the defined damage index DL is effective for nonlinear structural damage localization under earthquake excitations. When damage locations are determined, damage quantification can be performed based on Eq. (22). The damage quantification results for Cases 1-3 are shown in Figs. 11(a)-(c), respectively, and the results of Case 4 are described in Fig. 12. As observed from Figs. 11 and 12, the defined damage index DQ can clearly reflect the

occurrence of damage in Case 1 and Case 3 at the time instant of 6s, and the accumulation of

damage from 6s to 12s in Case 2, and from 8s to 12s in Case 4 at the 5th floor. These observations

are well matched with the predefined damage cases in Table 1. It can also be noticed that the

calculated DQ values for these cases are slightly fluctuant over time, which can be caused by the

varying hysteretic characteristics of the Bouc-Wen model due to the stiffness reductions. To better

quantify the severity of structural damage, the mean values of the calculated DQ are presented in

Table 2. The results indicate that the severity of damage under different cases is effectively

quantified by the proposed damage index. In summary, the identification results in the numerical

simulations demonstrate that the proposed approach is feasible for nonlinear structural damage

localization and quantification.

Table 2. Damage index values under different damage cases

Location	Case1	Case2	Case3	Case4	
	Second floor	Second floor	Second floor	Second floor	Fifth floor
DQ	0.17	0.17	0.23	0.17	0.23
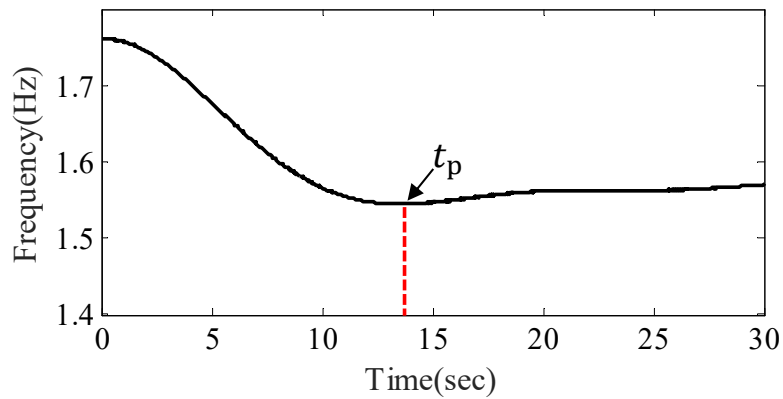
Fig. 7. The data point selected from the identified instantaneous frequency of the first main

component.

20
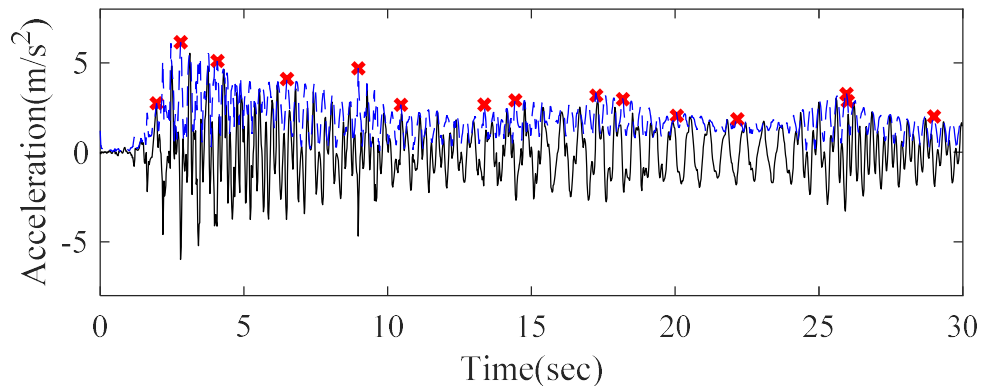
Fig. 8. Data points selected from the acceleration response at the top floor.
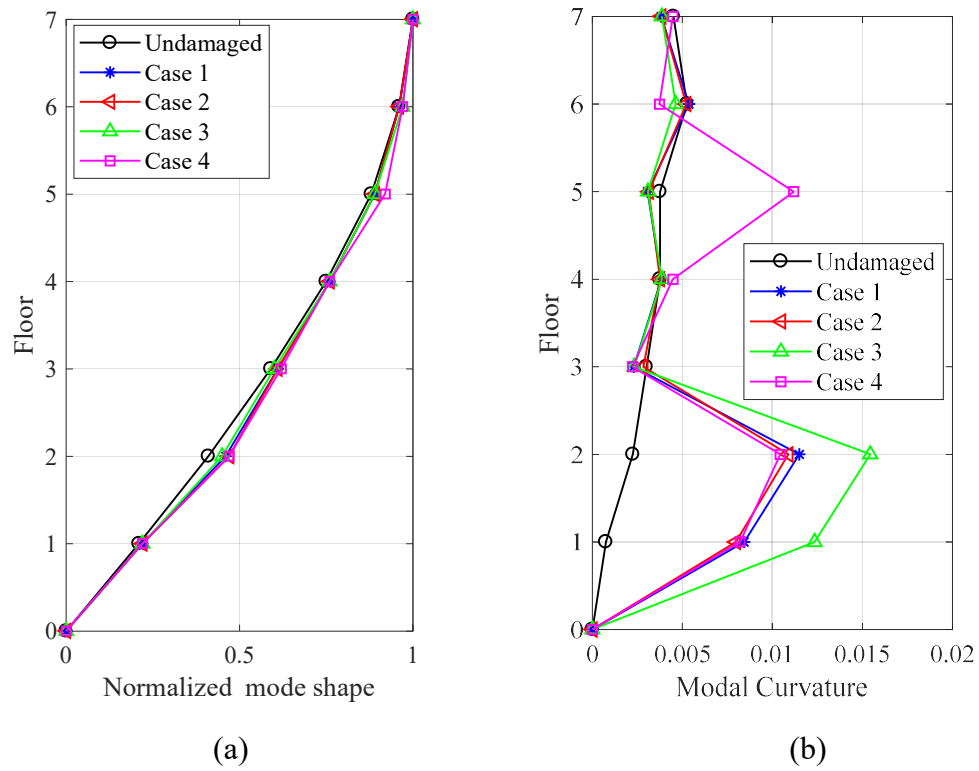

(a)   (b)

Fig. 9. The identified normalized mode shapes and modal curvtures under different damage cases:
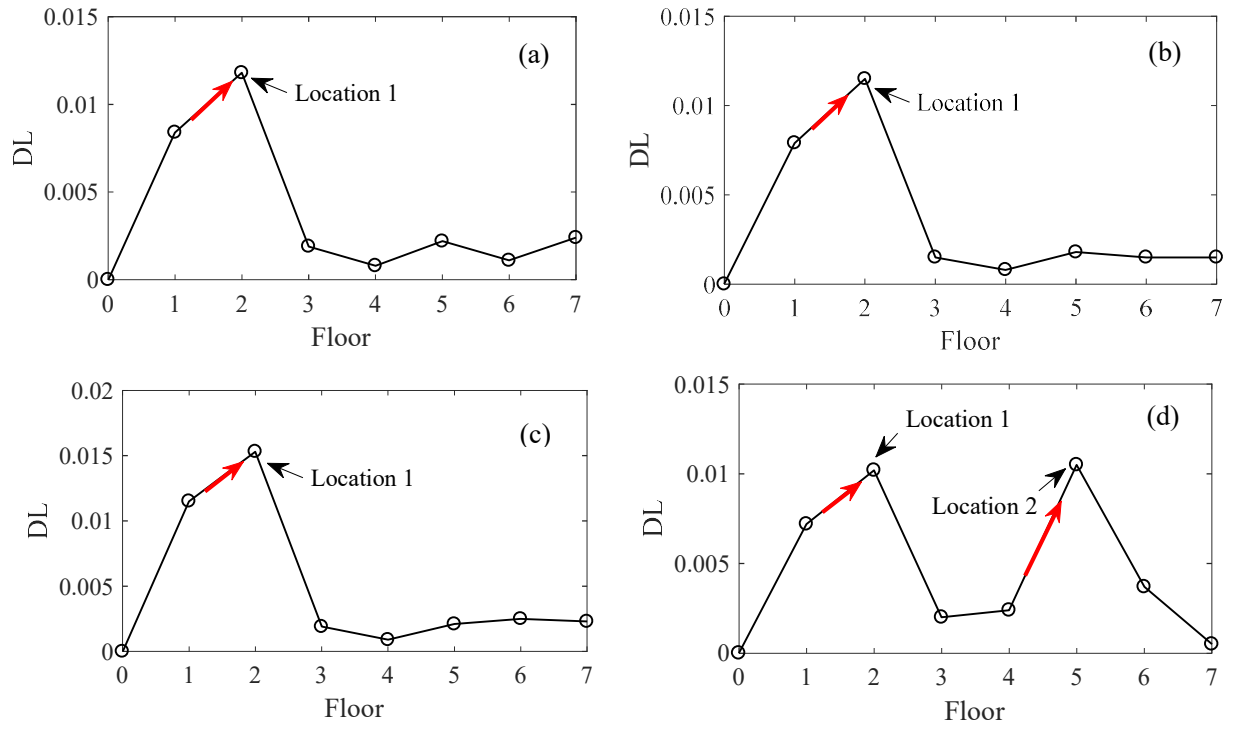
(a) Normalised mode shapes; (b) Modal curvatures.

Fig 10. Damage localization results based on the the defined damage index *DL*: (a) Case 1; (b) Case 2; (c) Case 3; (d) Case 4.
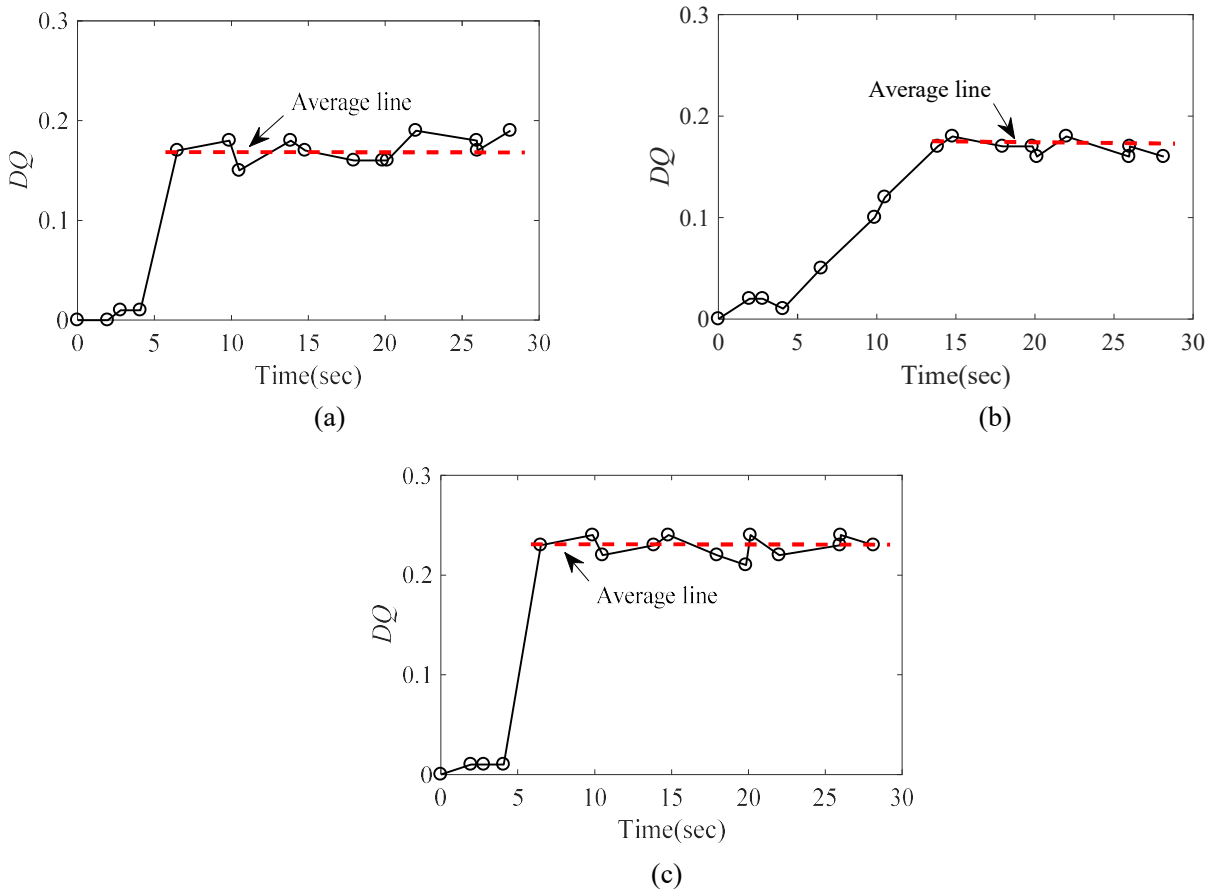
Fig. 11. Damage quantification results based on the defined damage index *DQ*: (a) Case 1; (b) Case 2; (c) Case 3.
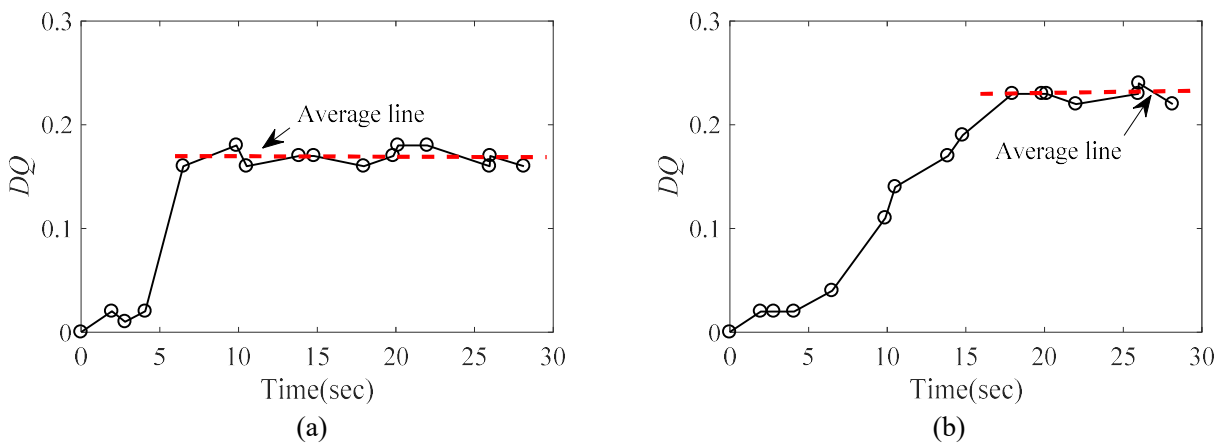
Fig. 12. Damage quantification results in Case 4: (a) The 2nd floor; (b) The 5th floor.

4. Experimental verification

To further examine the effectiveness of using the proposed approach for nonlinear structural damage identification, a 12-storey 1/10 scaled RC frame structure is built in the laboratory as shown in Fig. 13. The total height of the frame structure is 3.6m with 0.3m of each storey, and the dimension of the slab at each floor is 0.6m×0.6m. The detailed physical and geometrical parameters of the experimental testing structure can be found in [37]. The shake table tests were conducted at Tongji University and the testing data were shared for benchmark studies. During the tests, 23 accelerometers were employed to record the tri-axial dynamic responses of the RC structure under earthquake excitations. Totally, 61 cases were conducted to investigate the seismic performance of the RC structure under the various earthquake excitations. In this study, the measured dynamic responses under the single directional seismic loads are used for nonlinear structural damage identification, and the layout of seven accelerometers is shown in Fig. 14. The four cases selected for this study consider that the experimental structure was excited by the single directional earthquake excitations. The corresponding input ground motions in the shake table tests were the regenerated 1940 El Centro ground motion with four peak ground accelerations (PGA). The input time histories EQ_1, EQ_2, EQ_3 and EQ_4 are presented in Figs. 15(a)-(d), with the PGA values equal to 0.09g, 0.258g, 0.388g and 0.517g, respectively. The acceleration responses of the top floor under the four earthquake excitations are shown in Fig. 16, and their Fourier spectra are illustrated in Fig. 17. It can be observed from Fig. 17 that the fundamental natural frequencies of the RC structure under these four cases are different. This is mainly caused by the substantial damage in the RC structure during the testing. Before damage detection of the RC structure, the measured acceleration

responses under EQ_1 are used for modal identification of the initial linear structure. Based on the results of using the autoregressive power spectrum approach [38], the identified first and second natural frequencies of the RC structure are 3.98 Hz and 14.82Hz, respectively. According to the testing report [37], although no visible cracks are observed on the tested structure under EQ_2, the identified natural frequencies of the RC structure under EQ_2 are lower than those under EQ_1, as evidenced by Fig. 17. This phenomenon is likely due to the nonlinear dynamic behaviors of the tested structure during strong ground motion excitations, therefore the measured dynamic responses under EQ_2 can be considered as a reference structure with nonlinear dynamic characteristics. In this study, two damage cases when the tested RC structure is subjected to EQ_3 and EQ_4 excitations are studied herein for nonlinear damage identification.
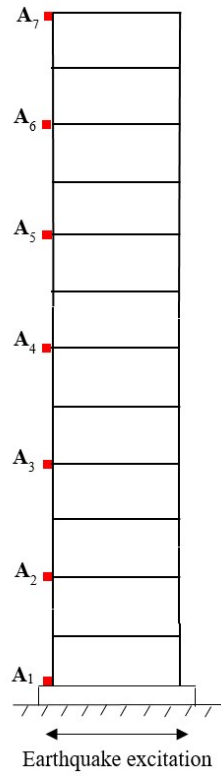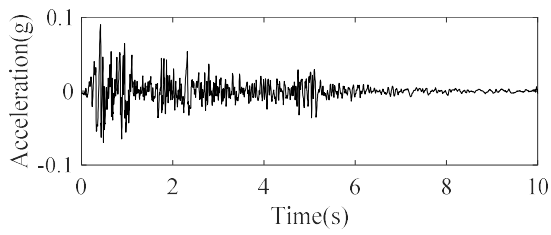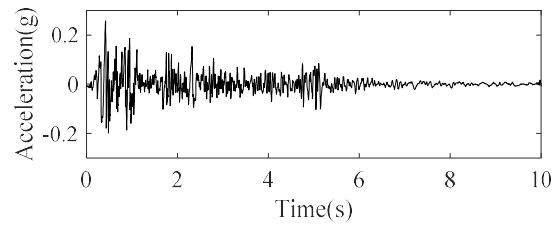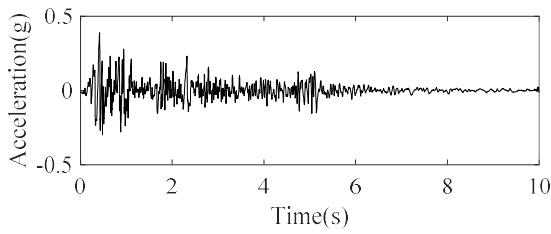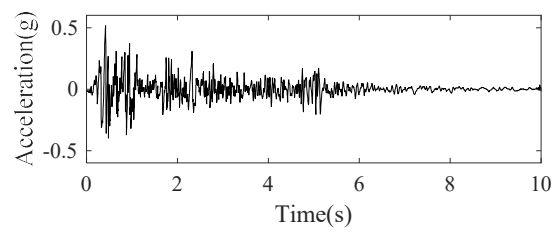

Fig 13. The experimental structure

Fig 14. The layout of accelerometer locations.

(a)	(b)
(c)	(d)

Fig 15. Four earthquake excitations: (a) EQ_1; (b) EQ_2; (c) EQ_3; (d) EQ_4.
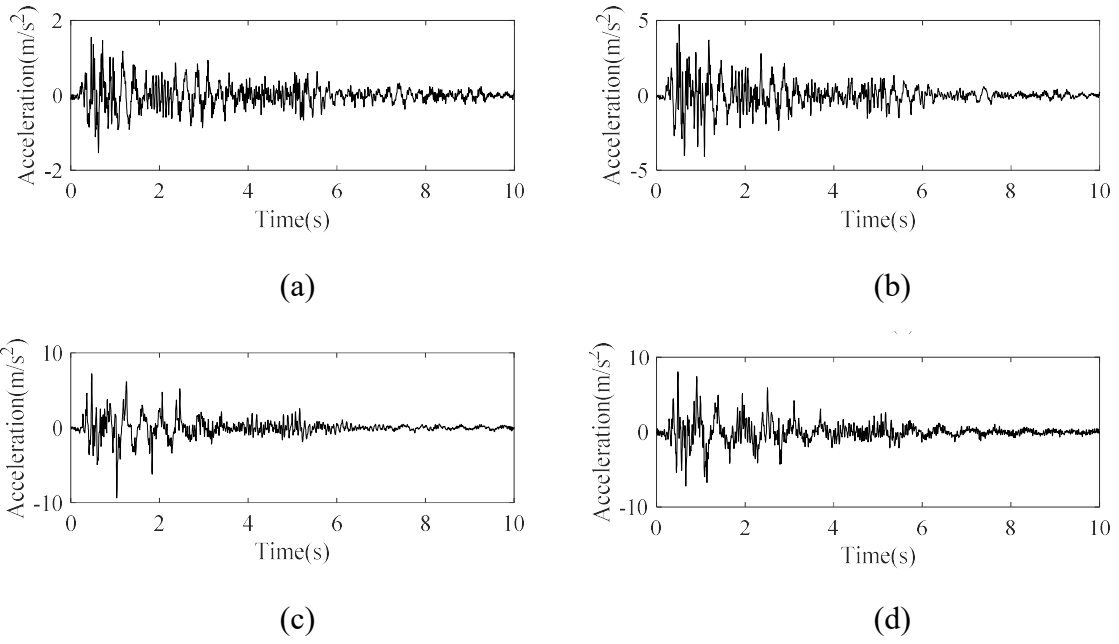
Fig 16. The recorded acceleration responses at the top floor under four seismic excitations: (a) EQ$_1$;

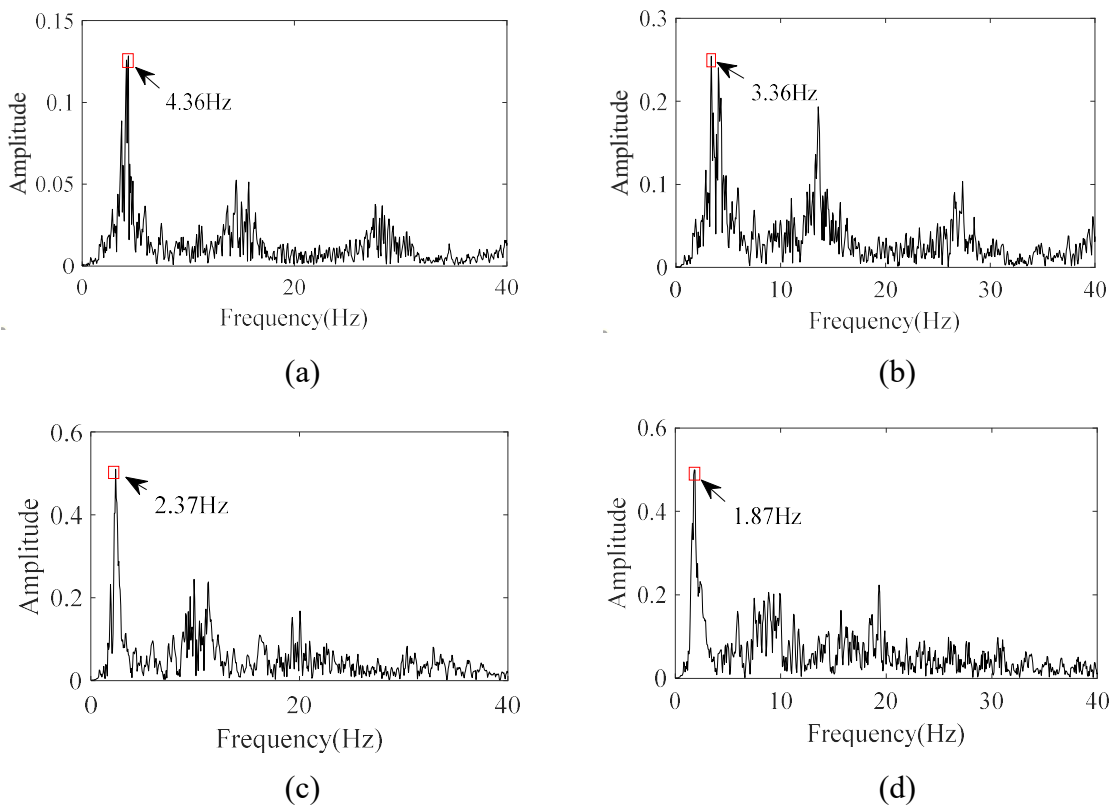(b) EQ$_2$; (c) EQ$_3$; (d) EQ$_4$.

Fig 17. The Fourier spectra of the recorded acceleration data at the top floor under four seismic

excitations: (a) EQ$_1$; (b) EQ$_2$; (c) EQ$_3$; (d) EQ$_4$.

For the building structure under EQ_3 and EQ_4 excitations, the instantaneous modal parameters of the fundamental mode are identified by using VMD method with Hilbert transform, and the decomposed fundamental mode of the measured acceleration signals at the top floor are shown in Fig. 18. The corresponding instantaneous fundamental frequencies of these two damage cases are also displayed. Then the damage indices are calculated based on the slowly-varying components of the identified instantaneous frequencies under the various earthquake excitations. In this experimental verification, the estimated modal curvatures of the fundamental mode are used for structural damage localization. The identified normalized mode shapes and the corresponding modal curvatures under three earthquake excitations EQ_2, EQ_3 and EQ_4 are shown in Fig. 19. Based on Eq. (21), the calculated damage index DL values of damage cases under EQ_3 and EQ_4 are displayed in Figs. 20(a) and (b), respectively. From Figs. 19 and 20, the results indicate that the fourth floor of the RC structure is identified as the location with the most severe damage during these two strong external excitations. Based on the testing report released by Tongji University [37], after the excitation of EQ_3, several vertical cracks were observed at the beams from the third floor to the sixth floor. The largest crack was located at the fourth floor, with a width of 0.15 mm approximately. Then, a stronger earthquake load EQ_4 was subsequently applied to the RC structure. The damage extent of the building structure was accumulated, and the range of the cracks was gradually extended to other floors. Hence, it can be shown that the identified results based on the proposed damage index DL are consistent with the testing observations. Once the damage locations of the tested RC structure are determined, the damage index DQ defined in Eq. (22) is further used to quantify the damage severity during the vibration period. Unlike the damage cases in the

numerical studies, for the tested RC structure, damage is substantially accumulated during the

strong earthquake excitations. In Figs. 16(c) and (d), 8 local peaks of the measured acceleration

responses at the top floor between 0s and 8s are selected for structural damage quantification. The

mean values of the calculated damage index DQ for the cases under EQ3 and EQ4 are listed in

Table 3. According to the experimental report [37], the tested RC structure has moderate damage

under EQ_3 (PGA=0.388g), and severe damage under EQ_4 (PGA=0.517g). As can be seen from

Table 3, the calculated damage index is capable of representing the severity of damage during two

earthquake excitations. Experimental results demonstrate that the proposed approach can be

successfully applied for structural damage quantification and localization in nonlinear systems.

Table 3. Damage quantification results under two different cases

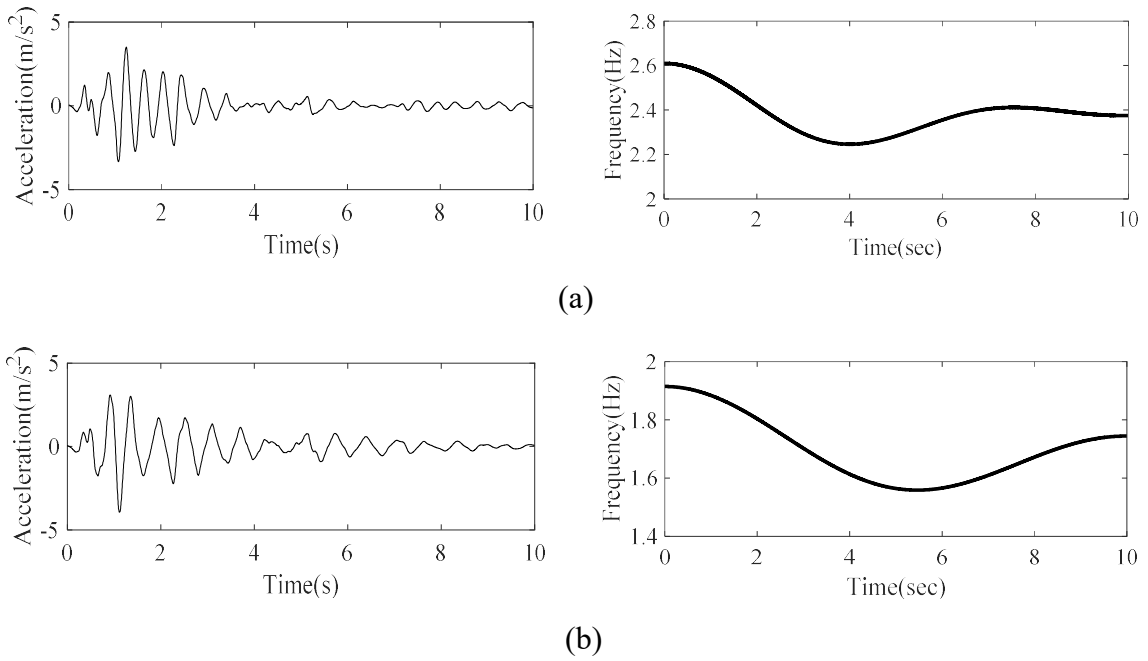|	EQ_3	EQ_4
DQ	0.51	0.72

(a)

(b)

Fig. 18. The first decomposed mode and the corresponding instantaneous frequencies of the

acceleration responses measured at the top floor under two different damage cases:
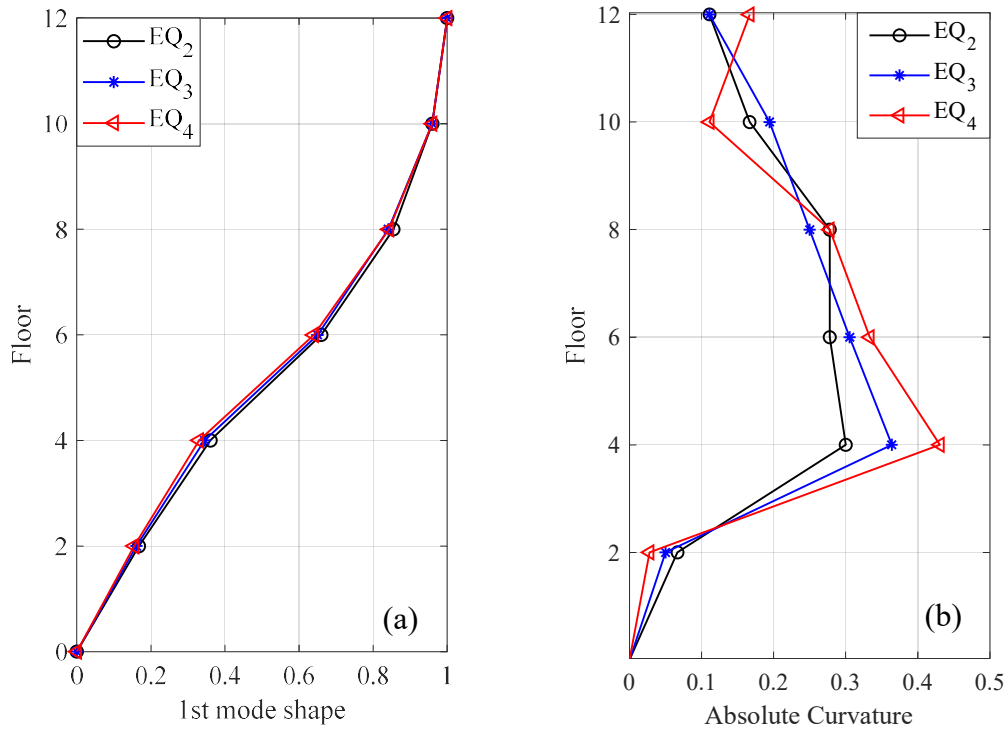
(a) EQ$_3$; (b) EQ$_4$.

Fig. 19. The identified normalzied mode shapes and the corresponding modal curvatures under two

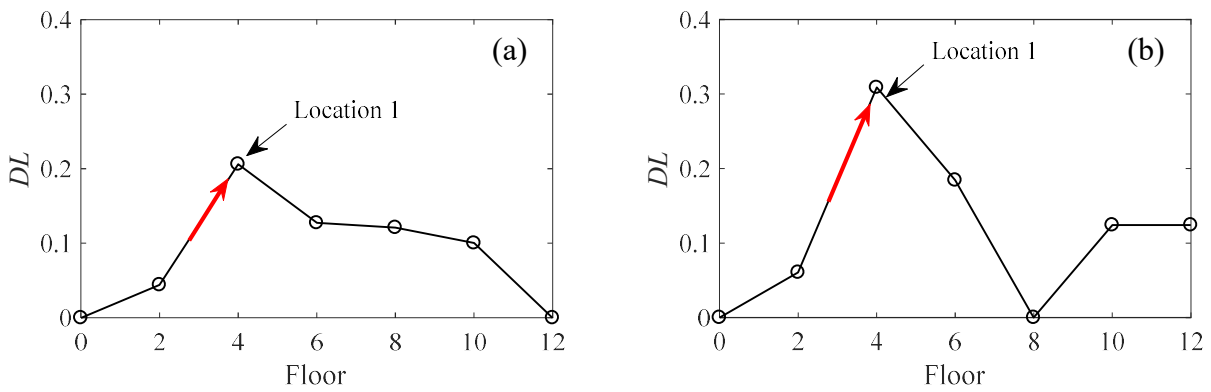different cases: (a) the normalized mode shapes; (b) the estimated modal curvatures.

Fig. 20. Damage localization based on the damage index *DL*: (a) EQ$_3$; (b) EQ$_4$.

5. Conclusions

This paper proposes using VMD with Hilbert transform for nonlinear structural damage

localization and quantification subjected to earthquake excitations. The measured dynamic responses from a nonlinear structure under earthquake excitations are adaptively decomposed into individual components by VMD method, and then the instantaneous modal parameters including instantaneous frequencies and mode shapes of the decomposed modes are identified by Hilbert transform. When these modal parameters are identified, two damage indices are defined for nonlinear structural damage localization and quantification, respectively. In the numerical studies, a seven-storey nonlinear building model with four damage cases under earthquake excitations is developed to examine the feasibility of the proposed method. In the experimental verifications, the proposed approach is further used for nonlinear structural damage identification with the shake table test data of a 12-storey scaled RC frame structure under seismic loads. The calculated damage index values identify the damage location and severity in the structures subjected to earthquake loads, which matches well the experimental testing observations.

Based on the damage identification results of the defined cases in both numerical studies and experimental validations, it can be concluded that the proposed approach can be successfully applied for nonlinear structural damage quantification and localization. However, it should be noticed that dynamic responses of all floors are required to be observed when using the proposed indices for damage detection of nonlinear structures. For the large-scale and complex structures, further studies on how to use a limited amount of structural responses for nonlinear structural damage detection can be conducted.

Acknowledgment

References

[1] Doebling S.W, Farrar C.R., Prime M.B., A summary review of vibration-based damage identification methods. *Shock and Vibration Digest* 1998; 30(2): 91-105.

[2] Li J., Hao H., Xia Y., Zhu H.P., Damage Detection of Shear Connections in Bridge Structures with Transmissibility in Frequency Domain. *International Journal of Structural Stability and Dynamics* 2014; 14(2): 1350061.

[3] Zhou X.Q., Huang W., Vibration-based Structural Damage Detection Under Varying Temperature Conditions. *International Journal of Structural Stability and Dynamics* 2013; 13 (5):1250082.

[4] Salawu O.S, Detection of structural damage through changes in frequency: a review. *Engineering Structures* 1997; 19(9): 718-723.

[5] Esfandiari A., Vahedi M., Enhanced Sensitivity for Structural Damage Detection Using Incomplete Modal Data. *International Journal of Structural Stability and Dynamics* 2018; 18 (4):1850054.

[6] Montejo L.A., Signal processing based damage detection in structures subjected to random excitations. *Structural Engineering and Mechanics* 2011; 40(6): 745-762.

[7] Yin T., Lam H.F., Chow H.M., Zhu H.P., Dynamic reduction-based structural damage detection of transmission tower utilizing ambient vibration data. *Engineering Structures* 2009; 31(9): 2009-2019.

[8] Zhu X.Q., Hao H., Damage Detection of RC Slabs Using Nonlinear Vibration Features. *International Journal of Structural Stability and Dynamics* 2009; 9(4): 687-709.

[9] Feldman M., Hilbert transform methods for nonparametric identification of nonlinear time-varying vibration systems. *Mechanical Systems and Signal Processing* 2014; 47(1-2): 66-77.

[10] Li J., Hao H., Substructure damage identification based on wavelet-domain response reconstruction. *Structural Health Monitoring* 2014; 13(4): 389-405.

[11] Ruzzene M., Fasana A., Garibaldi L., Piombo B., Natural frequencies and dampings identification using wavelet transform: Application to real data. *Mechanical Systems and Signal Processing* 1997, 11(2): 207-218.

[12] Xin Y., Hao H., Li J., Time-varying system identification by enhanced Empirical Wavelet Transform based on Synchroextracting Transform. *Engineering Structures* 2019; 196; 109313.

[13] Daubechies I., Lu J.F., Wu H.T., Synchrosqueezed wavelet transforms: An empirical mode decomposition-like tool. *Applied and Computational Harmonic Analysis* 2011; 30: 243-261.

[14] Huang N.E., Shen Z., Long S.R., Wu M.C., Shih H.H., Zheng Q., Yen N.C., Tung C., Liu H.H., The empirical mode decomposition and the Hilbert spectrum for nonlinear and non-stationary time-series analysis, *Proceedings of the Royal Society of London A: Mathematical, Physical and Engineering Sciences: The Royal Society* (1998) p. 903-995.

[15] Yang J.N., Lei Y., Pan S.W., Huang N., System identification of linear structures based on Hilbert-Huang spectral analysis, Part I: normal modes, *Earthquake Engineering and Structural Dynamics* 2003; 32:1443-67.

[16] Wang Z.C., Chen G.D., Recursive Hilbert-Huang Transform Method for Time-Varying Property Identification of Linear Shear-Type Buildings under Base Excitations. *Journal of Engineering Mechanics ASCE* 2012; 138: 631-639.

[17] Bao C.X., Hao H., Li Z.X., Zhu X.Q., Time-varying system identification using a newly improved HHT algorithm. *Computers & Structures* 2009; 87(23-24): 1611-1623.

[18] Dragomiretskiy K., Zosso D., Variational Mode Decomposition. *IEEE Transactions on Signal Processing* 2014; 62(3), 531-544.

[19] Zhang M., Jiang Z.N., Feng K., Research on variational mode decomposition in rolling bearings fault diagnosis of the multistage centrifugal pump. *Mechanical Systems and Signal Processing* 2017, 93(1): 460-493.

[20] Arrieta Paternina MR, Tripathy RK, Zamora-Mendez A, Dotta D, Identification of electromechanical oscillatory modes based on variational mode decomposition. *Electric Power Systems Research* 2019, 167: 71-85.

[21] Ni P.H., Li J., Hao H., Xia Y., Wang X.Y., Lee J.M., Jung K.H., Time-varying system identification using variational mode decomposition. *Structural Control and Health Monitoring* 2018; 25, e2175.

[22] Ditommaso R., Mucciarelli M., Ponzo F.C., Analysis of non-stationary structural systems by using a band-variable filter. *Bulletin of Earthquake Engineering* 2012; 10: 895-911.

[23] Chanpheng T., Yamada H., Katsuchi H., Sasaki E., Nonlinear features for damage detection on large civil structures due to earthquakes. *Structural Health Monitoring* 2012; 11(4): 482-488.

[24] Liu J.L., Wang Z.C. Ren W.X., Li X.X., Structural time-varying damage detection using synchrosqueezing wavelet transform. *Smart Structures and Systems* 2015; 15(1): 119-133.

[25] Xin Y., Hao H., Li J., Wang Z.C., Wan H.P., Ren W.X., Bayesian based nonlinear model updating using instantaneous characteristics of structural dynamic responses. *Engineering Structures* 2019; 183: 459-474.

[26] Bertsekas D.P., Constrained optimization and Lagrange Multiplier methods. *Computer Science and Applied Mathematics* 1982.

[27] Wang Z.C., Ren W.X., Chen G.D., Time-Varying Linear and Nonlinear Structural Identification with Analytical Mode Decomposition and Hilbert Transform. *Journal of Structural Engineering ASCE* 2013; 06013001-5.

[28] Wang Z.C., Xin Y., Ren W.X., Nonlinear structural model updating based on instantaneous frequencies and amplitudes of the decomposed dynamic responses. *Engineering Structures* 2015; 100(1): 189-200.

[29] He W.Y., He J., Ren W.X., The Use of Mode Shape Estimated from a Passing Vehicle for Structural Damage Localization and Quantification. *International Journal of Structural Stability and Dynamics* 2019; 19 (10):1950124.

[30] Cao M., Xu W., Ostachowicz W., Su Z.Q., Damage identification for beams in noisy conditions based on Teager energy operator-wavelet transform modal curvature. *Journal of Sound and Vibration* 2014; 333: 1543-1553.

[31] Ditommaso R., Ponzo F.C., Auletta G., Damage detection on frame structures: modal curvature evaluation using Stockwell Transform under seismic excitation. *Earthquake Engineering and Engineering Vibration* 2015; 14(2): 265-274.

[32] Dessi D., Camerlengo G., Damage identification techniques via modal curvature analysis: Overview and comparsion. *Mechanical Systems and Signal Processing* 2015; 53-53: 181-205.

[33] Wang Z.C., Geng D., Ren W.X., Chen G.D., Zhang G.F., Damage detection of nonlinear structures with analytical mode decomposition and Hilbert transform. *Smart Materials and Systems* 2015; 15(1): 1-13.

[34] Mazzoni S., Scott M.H., Mckenna F., Fenves G.L., et al., Open system for earthquake engineering simulation-user manual. Pacific Earthquake Engineering Research Center, University of California, Berkeley, California, 2006.

[35] Charampakis A.E., Koumousis V.K., Identification of Bouc-Wen hysteretic systems by a hybrid evolutionary algorithm. *Journal of Sound and Vibration* 2008; 314(3-5): 571-585.

[36] Lei Y., Wu Y., Li T., Identification of non-linear structural parameters under limited input and output measurements. *International Journal of Non-Linear Mechanics* 2012; 1411-1146.

[37] Lv X.L., Li P.Z., Chen Y.Q., Benchmark Test of a 12-storey Reinforced Concrete Frame Model on Shaking Table. Tongji University, Shanghai; 2004.

[38] Xin Y., Hao H., Li J., Operational modal identification of structures based on improved empirical wavelet transform. *Structural Control and Health Monitoring* 2019; 26: e2323.